Journal of Fluorescence, Vol. 3, No. 2, 1993

Review of Fluorescence Anisotropy Decay Analysis by Frequency–Domain Fluorescence Spectroscopy

Joseph R. Lakowicz,[1] Henryk Cherek,[1] Józef Kuśba,[1] Ignacy Gryczynski,[1] and Michael L. Johnson[2]

Received June 24, 1993; revised August 27, 1993

This didactic paper summarizes the mathematical expressions needed for analysis of fluorescence anisotropy decays from polarized frequency-domain fluorescence data. The observed values are the phase angle difference between the polarized components of the emission and the modulated anisotropy, which is the ratio of the polarized and amplitude-modulated components of the emission. This procedure requires a separate measurement of the intensity decay of the total emission. The expressions are suitable for any number of exponential components in both the intensity decay and the anisotropy decay. The formalism is generalized for global analysis of anisotropy decays measured at different excitation wavelengths and for different intensity decay times as the result of quenching. Additionally, we describe the expressions required for associated anisotropy decays, that is, anisotropy decays where each correlation time is associated with a decay time present in the anisotropy decay. And finally, we present expressions appropriate for distributions of correlation times. This article should serve as a reference for researchers using frequency-domain fluorometry.

KEY WORDS: Fluorescence anisotropy decays; frequency-domain fluorescence spectroscopy; review.

INTRODUCTION

Measurements of fluorescence anisotropy decays can reveal the size, shape, flexibility, and associative behavior of biological macromolecules [1–4]. Such decays are often measured in the time domain using time-correlated single-photon counting, as illustrated by the classic studies by Stryer and co-workers to reveal the dynamics of immunoglobulin proteins [5,6] and numerous more recent publications on the dynamics and hydrodynamics of macromolecules [7–15]. In recent years, the alternative method of frequency-domain (FD) fluorometry has become more widely used by the biophysics community. This use is the result of commercially available instrumentation and published results which indicated the usefulness of FD measurements for the resolution of complex fluorescence intensity [16–20] and anisotropy [21–25] decays. In fact, FD measurements provided the first resolution of three decay times for a rigid molecule [26], a phenomenon first predicted by F. Perrin in the 1930s.

The formalism for analysis of FD intensity decays has been described in detail in many publications [16–18,27,28]. In contrast, the equations needed for analysis of the FD anisotropy decays have not been presented in detail and are summarized here. Our presentation progresses from the simplest case of a single rotational correlation time and a single intensity decay time, to more complex cases which involve global analysis of data ob-

[1] Center for Fluorescence Spectroscopy and Department of Biological Chemistry, University of Maryland School of Medicine, 108 North Greene Street, Baltimore, Maryland 21201.

[2] Department of Pharmacology, University of Virginia, Box 448, Charlottesville, Virginia 22908.

1053-0509/93/0300-0103$07.00/0

tained for different excitation wavelengths and/or different decay times as the result of collisional quenching, to multiexponential intensity and anisotropy decays. Additionally, we described expressions for associated anisotropy decays and for correlation time distributions. We believe that the systematic approach, from the simpler to the more complex cases, provides the easiest manner to understanding the individual cases and allows an intuitive understanding that allows selection of the appropriate model for a given situation. The models described here are available as part of the program library at the Center for Fluorescence Spectroscopy (CFS), which can be accessed via the internet, and are available in PC versions. We note that anisotropy decay analysis can also be accomplished using the Globals Unlimited software package developed at the Laboratory for Fluorescence Dynamics (LFD), Urbana, Illinois. For convenience the mathematical terms are summarized under Nomenclature at the end of the text.

GENERAL THEORY

Expressions for Intensity and Anisotropy Decays

Assume that the sample is excited with vertically polarized light and that the emission is collected along an axis 90° away from the incident light. The observation polarizer may be oriented either parallel or perpendicular to the polarization of the incident light (Fig. 1). This experimental geometry can be related to other equivalent geometries as described previously [29]. The intensity decay can be described by a sum of exponential components,

$$I(t) = I_{\parallel}(t) + 2I_{\perp}(t) \tag{1}$$

$$I(t) = \sum_i \alpha_i e^{-t/\tau_i} = \sum_i \alpha_i e^{-\Gamma_i t} \tag{2}$$

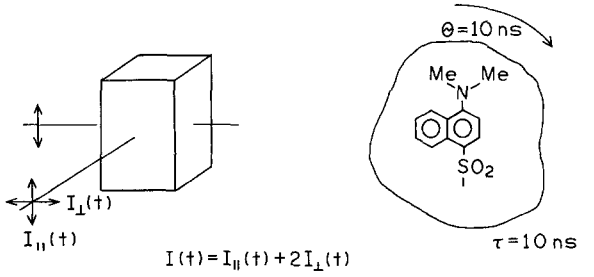

Fig. 1. Measurement of an anisotropy decay. The right side shows a hypothetical dansyl-labeled protein, with a lifetime and correlation time of 10 ns each.

where $I(t)$, $I_{\parallel}(t)$, and $I_{\perp}(t)$ are the decays of the toal, parallel, and perpendicular components of the emission. For the present paper we assume that the intensity decay can be described by the multiexponential model [Eq. (2)], where α_i are the preexponential factors, τ_i the decay times, $\Gamma_i = \tau_i^{-1}$ the decay rates, and n the number of decay times. We note that intensity decays can be nonexponential (i.e., not a sum of exponential components) due to a distribution of decay times [17,28] or transient effects in quenching [18], to name a few. Nonetheless, for the anisotropy analysis it is necessary only to have an expression which accurately describes the intensity decay. In this respect the multiexponential model is very powerful, and based on our experience, it is always possible to model the intensity decay data with the multiexponential model [Eq. (2)].

The anisotropy decay is also assumed to be a sum of exponentials,

$$r(t) = \sum_j r_0 g_j e^{-t/\theta_j} = \sum_j r_{0j} e^{-6R_j t} \tag{3}$$

where $\theta_j = (6R_j)^{-1}$ are the rotational correlation times, R_j the rotational rates, g_j the fractional amplitudes for each component in the anisotropy decay ($\Sigma_j g_j = 1.0$), $r_{0j} = r_0 g_j$ the amplitudes of each component in the anisotropy decay, and r_0 the total anisotropy observed at $t = 0$. In those cases where the instrumental time resolution is adequate to detect the fastest amount in the anisotropy decay, r_0 is equal to the anisotropy observed in the absence of rotational motion during the lifetime of the excited state.

The polarized components of the intensity decay are related to anisotropy decay by

$$I_{\parallel}(t) = \frac{1}{3} I(t) [1 + 2r(t)] \tag{4}$$

$$I_{\perp}(t) = \frac{1}{3} I(t) [1 - r(t)] \tag{5}$$

Measurement of an anisotropy decay using time-domain data typically requires taking the difference between the two larger quantities $I_{\parallel}(t)$ and $I_{\perp}(t)$. This is illustrated in Fig. 2, where we show hypothetical data for a spherical protein. In this example we assume that the intensity decay was a single exponential with a decay time of 10 ns and that the fluorophore is rigidly bound to the protein, which rotates with a 10-ns correlation time. While the total intensity decay $I(t) = I_{\parallel}(t) + 2I_{\perp}(t)$ is a single exponential (left), the polarized components $I_{\parallel}(t)$ and $I_{\perp}(t)$ display more complex intensity decays [Eqs. (4) and (5)]. In particular, the parallel component shows an initial rapid decay due to rotation of the transition moment

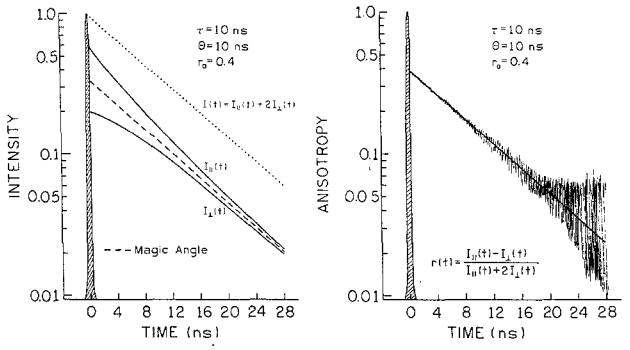

Fig. 2. Time-domain measurements of an anisotropy decay. For these simulated data we assumed a decay time (τ) of 10 ns and a correlation time of 10 ns.

of the fluorophore out of the vertical orientation (assuming $r_0 > 0$). The perpendicular component of the anisotropy decays more slowly because this component is populated by rotation from the vertical component. At longer times the decay becomes identical and independent of the initial photoselected difference due to rotational diffusion.

In time-domain measurements of an anisotropy decay, one takes the difference between the polarized intensity decays [Eqs. (4) and (5) and Fig. 2, right], normalized by the total intensity decay. Typically, there is considerable uncertainty in the anisotropy decay (Fig. 2, right) because these values are calculated from the difference two larger values.

FD anisotropy decays can be measured in a similar manner, by separate measurements of the phase and modulation of the parallel and perpendicular components [30]. Such measurements of the frequency response of each polarized component are illustrated in Figs. 3 and 4. The phase angles of the parallel component are expected to be shorter than that of the total decay (- - -) because the vertically oriented molecules rotate out of the vertical orientation (Fig. 3). In contrast, the horizontal component displays larger phase angles because this component is populated in part by rotational diffusion. Similarly, we expect the modulated amplitude of the vertical component to be larger, because of its more rapid decay (Fig. 3).

One can imagine two methods to use the FD measurements to determine the anisotropy decay. One could measure the phase and modulation of the polarized components, relative to the modulated excitation, as shown in Fig. 4. One could then take the differences (and ratios) and analyze the resulting data file. However, the uncertainties in the individual measurements ($\parallel$ and $\perp$) would both contribute to the difference and ratio values.

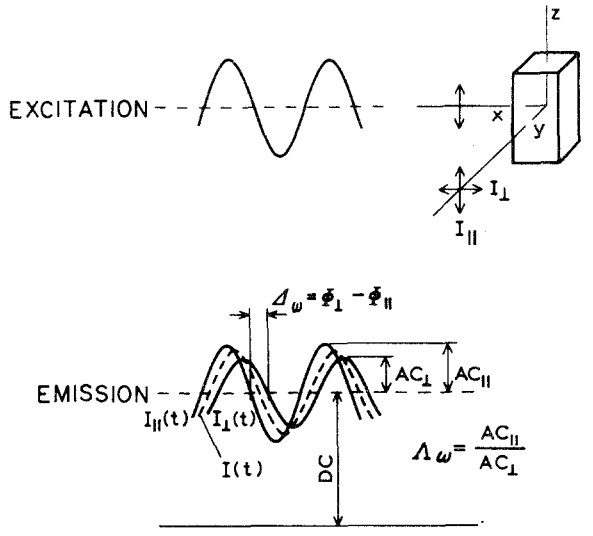

Fig. 3. FD measurement of an anisotropy decay. For simplification, all *DS* components (bias) in this figure are taken as equal ($DC_\parallel = DC_\perp$). In real measurements the *DC* components can be different. See the text [Eqs. (12)–(18)] for a general description.

For measurements of the anisotropy decay we prefer to measure directly the phase difference (Δ) between the polarized components of the emission and the ratio of the polarized and modulated components of the emission (Λ), as suggested in the pioneering paper by Weber [31] . Such measurements are illustrated in Fig. 4 (bottom). By rotation of the emission polarizer, one directly measures the phase difference Δ between the vertical and the horizontal components of the emission. Simultaneously, one measures the amplitudes of the modulated components of the emission. This results in the familiar form of the FD anisotropy data shown in Fig. 4 (bottom panels). We feel that these difference measurements provide the best approach for quantifying the small difference between the polarized components of the emission. Because this difference measurement does not determine the phase and modulation of the emission, relative to the modulated excitation, these data do not determine the intensity decay. Consequently, the intensity decay is determined by separate measurement of the phase modulation of the total emission, relative to the modulated excitation, using magic angle polarization conditions. This decay is illustrated in Fig. 4 (top; ---).

Analysis of FD Data

In the FD the intensity decays are determined from the phase (ϕ_ω) and modulation (m_ω) of the emission,

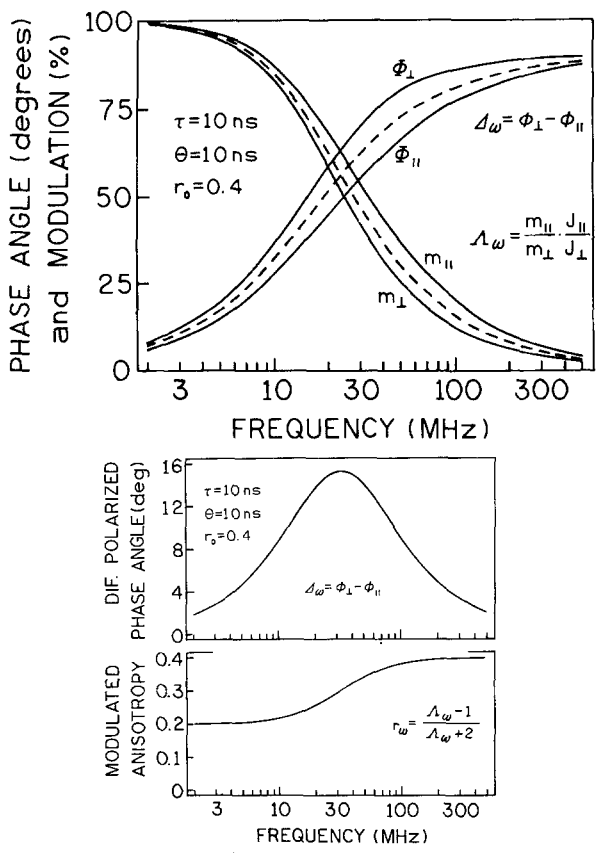

Fig. 4. Simulated FD data for an anisotropy decay, τ = 10 ns and θ = 10 ns. The top panel shows the phase and modulation of the polarized components of the emission, relative to the modulated excitation. The bottom panels show the differential measurements of the phase angle difference (Δ_ω) and modulated amplitude ratio (Λ_ω or r_ω).

relative to scattered light, each measured over a range of modulation frequencies (ω), where ω is in radians per second. These measured values are compared with values calculated (c) for an assumed intensity decay law ($\phi_{c\omega}$ and $m_{c\omega}$) using

$$\phi_{c\omega} = \arctan (N_\omega/D_\omega) \tag{6}$$

$$m_{c\omega} = \frac{1}{J}\sqrt{N_\omega^2 + D_\omega^2} \tag{7}$$

where

$$N_\omega = \int_0^\infty I(t) \sin\omega t\, dt \tag{8}$$

$$D\omega = \int_0^\infty I(t) \cos \omega t\, dt \tag{9}$$

$$J = \int_0^\infty I(t)\, dt \tag{10}$$

The parameters describing the intensity decay [α_i and τ_i from Eq. (2)] are determined by minimizing the differences between the measured and the calculated values of ϕ_ω and m_ω using

$$\chi_R^2 = \frac{1}{\nu}\sum_\omega \left(\frac{\phi_\omega - \phi_{c\omega}}{\delta\phi}\right)^2 + \frac{1}{\nu}\sum_\omega \left(\frac{m_\omega - m_{c\omega}}{\delta m}\right)^2 \tag{11}$$

where ν is the number of degrees of freedom and $\delta\phi$ and δm are the experimental uncertainties of the measurements.

Anisotropy Decay Analysis

Similar expressions apply for analysis of anisotropy decays from the FD data. In this case the experimental quantities are the phase angle difference between the perpendicular ($\phi_\perp$) and the parallel ($\phi_\parallel$) components of the polarized emission (Fig. 3),

$$\Delta_\omega = \phi_\perp - \phi_\parallel = \arctan\left(\frac{D_\parallel N_\perp - N_\parallel D_\perp}{N_\parallel N_\perp + D_\parallel D_\perp}\right) \tag{12}$$

and the ratio of the parallel and perpendicular AC components of the modulated emission,

$$\Lambda_\omega = \frac{AC_\parallel}{AC_\perp} = \frac{\sqrt{N_\parallel^2 + D_\parallel^2}}{\sqrt{N_\perp^2 + D_\perp^2}} \tag{13}$$

where

$$N_p = \int_0^\infty I_p(t) \sin \omega t\, dt \tag{14}$$

$$D_p = \int_0^\infty I_p(t) \cos \omega t\, dt \tag{15}$$

The subscript p indicates either the parallel or the perpendicular component at the emission. These expressions were presented previously in Refs. 30 and 31 in somewhat different forms. It should be noted that the N_p and D_p values are not normalized by the total intensity, as was the case for analysis of the intensity decay [Eqs. (8)–(10)].

We note that Λ_ω is the ratio of the AC components, and not the ratio $m_\parallel/m_\perp$ of the modulations of the polarized components. The modulations of the polarized components are

$$m_\parallel = \frac{AC_\parallel}{DC_\parallel m_{exc}} = \frac{1}{J_\parallel}\sqrt{N_\parallel^2 + D_\parallel^2} \tag{16}$$

$$m_\perp = \frac{AC_\perp}{DC_\perp m_{exc}} = \frac{1}{J_\parallel}\sqrt{N_\perp^2 + D_\perp^2} \tag{17}$$

where m_{exc} denotes the modulation of the incident light and $J_\parallel$ and $J_\perp$ are the steady-state intensities of the polarized components

$$J_p = \int_0^\infty I_p(t)\, dt \tag{18}$$

It is seen from Eqs. (13) and (16) that

$$\Lambda_\omega = \frac{m_\parallel}{m_\perp}\frac{J_\parallel}{J_\perp} \tag{19}$$

The meaning of Λ_ω is comparable to that of the intensity ratio of the polarized steady-state intensities. We prefer to present this observable as the modulated anisotropy [22],

$$r_\omega = \frac{\Lambda_\omega - 1}{\Lambda_\omega + 2} \tag{20}$$

The modulated anisotropy has properties of both the steady-state anisotropy (r) and the fundamental anisotropy (r_0). More specifically, at modulation frequencies which are low compared to the correlation time(s), r_ω approaches r. At modulation frequencies much higher than the correlation time(s), r approaches r_0.

The parameters describing the anisotropy decay are obtained by a nonlinear least-squares analysis of the data [32–34], by the minimization of the goodness-of-fit indicator

$$\chi_R^2 = \frac{1}{\nu}\sum_\omega\left(\frac{\Delta_\omega - \Delta_\omega}{\delta\Delta}\right)^2 + \frac{1}{\nu}\sum_\omega\left(\frac{\Lambda_\omega - \Lambda_{c\omega}}{\delta\Lambda}\right)^2 \tag{21}$$

where $\delta\Delta$ and $\delta\Lambda$ are the uncertainties in the data and ν is the number of degrees of freedom. For calculation of χ_R^2 we have chosen values of $\delta\Delta$ and $\delta\Lambda$ to give approximately equal weight to the differential phase (Δ_ω) and modulation (Λ_ω) data.

Method of Measurement

Determination of an anisotropy decay requires knowledge of the total intensity decay and the difference between the parallel and the perpendicular components of the decay. In the time domain this is usually accomplished by measuring the time-dependent decays of the parallel and perpendicular components of the emission, $I_\parallel(t)$ and $I_\perp(t)$. The weighted sum [$I_\parallel(t) + 2I_\perp(t)$, Eq. (1)] can be analyzed to obtain the intensity decay law. The difference [$I_\parallel(t) - I_\perp(t)$] can be analyzed to recover $r(t)$ [35–37], although some researchers prefer to analyze simultaneously the measured decays $I_\parallel(t)$ and $I_\perp(t)$ in terms of the intensity and anisotropy decay parameters [37,38].

The FD anisotropy determination also requires two separate measurements. Although we have chosen not to do so, it is possible to measure independently the frequency response of $I_\parallel(t)$ and $I_\perp(t)$, each relative to scattered light, and to use these frequency responses to recover the anisotropy decay [30]. However, this approach requires calculation of the differences (Δ_ω and Λ_ω) between larger numbers, and hence a higher uncertainty in the value of Δ_ω and Λ_ω. Hence, we first measure the intensity decay using magic angle or rotation-free polarization conditions [39, 40]. These data (ϕ_ω and m_ω) are used to recover the intensity decay law $I(t)$ in terms of α_i and τ_i. These parameters are held constant in the subsequent anisotropy analysis. The second measurement is then a difference or ratio measurement between the polarized components of the emission, to determine Δ_ω and Λ_ω, respectively. The data are then analyzed in terms of Eqs. (14)–(20) to recover the anisotropy decay law.

ANISOTROPY DECAY MODELS

A large number of anisotropy decay models are possible. For clarity and ease of presentation, we use the term DIFXYZ to indicate an anisotropy decay model. The letters DIF originate with the term DIFferential phase, as used by Weber [31]. The letters X and Y refer to the number of decay times in the intensity decay and in the anisotropy decay, correlation time, respectively. The letter Z is used to indicate whether the value of r_0 is assumed to be known (Z = R) or unknown (Z = O). Hence, DIF23R refers to a model in which the intensity decay is represented as a double exponential, the anisotropy data are analyzed in terms of three correlation times, and the total anisotropy r_0 is assumed to be known. Recall that the intensity decay is measured separately and that the α_i and τ_i values are held fixed during the anisotropy analysis. Hence, the DIF23R anisotropy analysis has five variable parameters, three θ_j and two g_j values. In general, it is preferable if the value of r_0 is known, as this reduces the number of variable parameters. If r_0 is not known, then there are six floating parameters in the DIF230 model. However, we caution that if one assumes a value of r_0, and it is incorrect, then the least-squares analysis will introduce extra correlation time into the anisotropy decay. Unless indicated otherwise the de-

cay times and correlation times are not associated [41–43].

We now present some specific anisotropy decay models. Of course, it is possible to write generalized formula. However, we frequently find it useful to examine the specific models, particularly as these models are being coded into the data analysis program.

Calculation of Δ_ω and Λ_ω requires knowledge of $N_\parallel$, $N_\perp$, $D_\parallel$, and $D_\perp$ [Eqs. (12)–(15)]. These terms are given by

$$N_\parallel = \frac{1}{3}(A + 2B) \tag{22}$$

$$N_\perp = (A - B) \tag{23}$$

$$D_\parallel = \frac{1}{3}(C + 2D) \tag{24}$$

$$D_\perp = \frac{1}{3}(C - D) \tag{25}$$

where

$$A = \sum_i \frac{\alpha_i \omega}{\omega^2 + \Gamma_i^2} \tag{26}$$

$$B = \sum_i \alpha_i \omega \sum_j \frac{r_{0j}}{\omega^2 + (\Gamma_i + 6R_j)^2} \tag{27}$$

$$C = \sum_i \frac{\alpha_i \Gamma_i}{\omega^2 + \Gamma_i^2} \tag{28}$$

$$D = \sum_i \alpha_i \sum_j \frac{r_{0j}(\Gamma_i + 6R_j)}{\omega^2 + (\Gamma_i + 6R_j)^2} \tag{29}$$

Single-Exponential Intensity and Anisotropy Decay (DIF110)

The simplest case is when both the intensity and the anisotropy decay as single exponentials. In this case the transforms are given by

$$N_\parallel = \frac{1}{3}\left[\frac{\omega}{(\omega^2+\Gamma^2)} + \frac{2r_0\omega}{\omega^2+(\Gamma+6R)^2}\right] \tag{30}$$

$$N_\perp = \frac{1}{3}\left[\frac{\omega}{(\omega^2+\Gamma^2)} - \frac{r_0\omega}{\omega^2+(\Gamma+6R)^2}\right] \tag{31}$$

$$D_\parallel = \frac{1}{3}\left[\frac{\Gamma}{(\omega^2+\Gamma^2)} + \frac{2r_0(\Gamma + 6R)}{\omega^2+(\Gamma+6R)^2}\right] \tag{32}$$

$$D_\perp = \frac{1}{3}\left[\frac{\Gamma}{(\omega^2+\Gamma^2)} - \frac{r_0(\Gamma+6R)}{\omega^2+(\Gamma+6R)^2}\right] \tag{33}$$

For this simple case it is practical to reduce these expressions to a simpler expression which directly yields Δ_ω and Λ_ω. Using Eqs. (30)–(33) and (12)–(15), these values are given by

$$\tan\Delta_\omega = \frac{3\omega\tau r_0(6R\tau)}{m_0(1 + \omega^2\tau^2) + (2 + r_0)(GR\tau) + (6R\tau)^2} \tag{34}$$

$$\Lambda_\omega = \sqrt{\frac{[(1+2r_0)\omega\tau]^2 + [1+2r_0 + 6R\tau]^2}{[(1-r_0)\omega\tau]^2 + [1-r_0 + 6R\tau]^2}} \tag{35}$$

where $m_0 = (1 + 2r_0)(1 - r_0)$. Equation (34) was described originally by Weber [31]. In this simple model the variable terms are θ and r_0. If the value of r_0 is known, then there is only a single variable θ in the DIF11R model. In general, both the intensity and the anisotropy decays of biological molecules are multiexponential, so this simple case occurs only infrequently. The main use of the single-correlation time program is as a starting point for further analysis by the multiexponential models.

Multiexponential Intensity and Anisotropy Decay

A more common occurrence is for the sample to display multiexponential intensity decay, for which one wishes to recover multiple correlation times. In the case of a double-exponential intensity decay and the presence of three correlation times, the transfers are

$$A = \frac{\alpha_1\omega}{\omega^2+\Gamma_1^2} + \frac{\alpha_2\omega}{\omega^2+\Gamma_2^2} \tag{36}$$

$$B = \alpha_1\omega\left[\frac{r_{01}}{\omega^2+(\Gamma_1+6R_1)^2} + \frac{r_{02}}{\omega^2+(\Gamma_1+6R_2)^2} + \frac{r_{03}}{\omega^2+(\Gamma_1+6R_3)^2}\right]$$

$$+ \alpha_2\omega\left[\frac{r_{01}}{\omega^2+(\Gamma_2+6R_1)^2} + \frac{r_{02}}{\omega^2+(\Gamma_2+6R_2)^2} + \frac{r_{03}}{\omega^2+(\Gamma_2+6R_3)^2}\right] \tag{37}$$

$$C = \frac{\alpha_1\Gamma_1}{\omega^2+\Gamma_1^2} + \frac{\alpha_2\Gamma_2}{\omega^2+\Gamma_2^2} \tag{38}$$

$$D = \alpha_1\left[\frac{r_{01}(\Gamma_1 + 6R_1)}{\omega^2+(\Gamma_1+6R_1)^2} + \frac{r_{02}(\Gamma_1 + 6R_2)}{\omega^2+(\Gamma_1+6R_2)^2} + \frac{r_{03}(\Gamma_1 + 6R_3)}{\omega^2+(\Gamma_1+6R_3)^2}\right]$$

$$+ \alpha_2\left[\frac{r_{01}(\Gamma_2+6R_1)}{\omega^2+(\Gamma_2+6R_1)^2} + \frac{r_{02}(\Gamma_2+6R_2)}{\omega^2+(\Gamma_2+6R_2)^2} + \frac{r_{03}(\Gamma_2+6R_3)}{\omega^2+(\Gamma_2+6R_3)^2}\right] \tag{39}$$

During the least-squares analysis programs, it is assumed that the intensity decay law, that is, the values of α_i and τ_i, are known from a separate measurement. Hence, the variable parameters are the three correlation times (θ_j) and anisotropy amplitudes (r_{0j}). Resolution of these correlation times is a difficult task, particularly if the largest and smallest correlation times differ by less than a factor of 2.0. A successful and/

or unique three-correlation time analysis requires data over a wide range of frequencies. A multiexponential intensity decay is desirable because this extends the range of measurable frequencies. For instance, the shortest component in the intensity decay dominates the signal at higher modulation frequencies, allowing measurements to be made to higher frequencies before the modulation of the emission becomes too small for reliable measurements. Also, three correlation times are most easily recovered when the correlation times are widely spaced, as often occurs for membrane- or protein-bound probes. The ability to detect three correlation times for small rigid and asymmetric molecule is probably aided by slip rotation diffusion, which results in a greater range of correlation times than can be expected for hydrodynamic diffusion.

Resolution of three closely spaced correlation time is a difficult task, which often requires the use of multiple measurements, such as in the presence of quenching to vary the relationships among τ_i, θ_j, and ω [44]. These methods are described below in more detail.

For the analysis of complex anisotropy decays, it is essential to consider correlation between the parameters. Correlation allows the value of one parameter (r_{0j} or θ_j) to vary, without changing the value of χ^2_R, by a compensating change in another parameter value [33,34]. We found that the uncertainties estimated from the usual assumptions of nonlinear least squares (uncorrelated parameters) are severalfold smaller than those found by the method of Johnson [33,34], which estimates the range of parameters consistent with the data by a coarse search of the χ^2_R-parameter surface. In the comparison of complex anisotropy decays, we are often interested in the range of values, for a given parameter, which are consistent with the data. For instance, suppose that the sample is a protein which displays three correlation times (θ_1, θ_2, and θ_3) and that the solution conditions are changed and the protein again displays three correlation times (θ'_1, θ'_2, and θ'_3). Suppose that the value of θ_3 and θ'_3 represent overall rotational differences and that these values are slightly different. One may wish to determine whether this difference is firmly supported by the data or whether the values are within the uncertainty range for correlated parameters. For this purpose of finding the maximum range of parameter values consistent with the data, we prefer the more rigorous method of examining the χ^2_R surfaces [26,44,45]. Each parameter is held at fixed values around the expected value, and the χ^2_R minimization algorithm is run again to allow the remaining parameters to vary. If χ^2_R is not changed significantly, then the altered parameter value is still consistent with the data. If χ^2_R is elevated significantly, then the altered parameter value is not consistent with the data, irregardless of the extent of correlation. This procedure is rather time-consuming because it requires multiple analyses and typically requires interactive input from the individual performing the analysis. However, we believe that the flatness or steepness of the χ^2_R provides an unambiguous evaluation of the confidence interval for each parameter. The 67% confidence interval is given by the point where the value of χ^2_R increases by the F statistic for the degrees of freedom for the experiment [32,46].

Multiexponential Anisotropy Decay with a Known r_0

Frequently the total or fundamental anisotropy (r_0) can be determined from a separate experiment, such as measurement of the steady-state anisotropy in a vitrified solvent, as has been used for many years [47,48]. Most fluorophores, and even solvent-sensitive fluorophores such as tryptophan and indole, display wavelength regions of constant anisotropy where r_0 can be measured in the frozen solution, and where the temperature-dependent solvent effects are not likely to alter r_0 [49,50]. If r_0 is known, then it can be constrained in the anisotropy decay analysis. This constraint generally increases the stability and/or resolution of the analysis because the program is forced to account for the total anisotropy and because there is one fewer variable parameter. Knowledge of r_0 is particularly advantageous when a rapid correlation time is present in the anisotropy decay, in which case the apparent anisotropy at $t = 0$ can be less than r_0 due to the limited time resolution of most instrumentation. However, it should be noted that fixing r_0 at a value larger than the actual value will result in the appearance of a rapid correlation time to account for the excess anisotropy.

If the value of r_0 is known, there are $(m-1)$ amplitudes (g_j). The A and C terms do not contain the anisotropy decay components and are the same as Eqs. (26) and (28). The other terms are given by

$$B = r_0 \sum_i \alpha_i \sum_{j=1}^{m-1} \frac{\omega g_j}{\omega^2 + (\Gamma_i + 6R_j)^2} + r_0 \sum_i \frac{\omega \alpha_i g_m}{\omega^2 + (\Gamma_i + 6R_m)^2} \tag{40}$$

$$D = r_0 \sum_i \alpha_i \sum_{j=1}^{m-1} \frac{\alpha g_j (\Gamma_i + 6R_j)}{\omega^2 + (\Gamma_i + 6R_j)^2} + r_0 \sum_i \frac{\alpha g_m (\Gamma_i + 6R_j)}{\omega^2 + (\Gamma_i + 6R_m)^2} \tag{41}$$

In these expressions one of the g_j values is determined from the remainder by $\sum_j g_j = 1.0$. In particular, we calculate the last term of the sum using $g_m = 1 - \sum_{j \neq m} g_j$.

Suppose that the sample displays two decay times and two correlation times and r_0 is known (DIF22R). Once again, the A and C terms are given by Eqs. (26) and (28). The other terms are

$$B = r_0\alpha_1\omega\left[\frac{g_1}{\omega^2+(\Gamma_1+6R_1)^2} + \frac{(1-g_1)}{\omega^2+(\Gamma_1+6R_2)^2}\right] + r_0\alpha_2\omega\left[\frac{g_1}{\omega^2+(\Gamma_2+6R_1)^2} + \frac{(1-g_1)}{\omega^2+(\Gamma_2+6R_2)^2}\right] \quad (42)$$

$$D = r_0\alpha_1\left[\frac{g_1(\Gamma_1+6R_1)}{\omega^2+(\Gamma_1+6R_1)^2} + \frac{(1-g_1)(\Gamma_1+6R_2)}{\omega^2+(\Gamma_1+6R_2)^2}\right] + r_0\alpha_2\left[\frac{g_1(\Gamma_2+6R_1)}{\omega^2+(\Gamma_2+6R_1)^2} + \frac{(1-g_1)(\Gamma_2+6R_2)}{\omega^2+(\Gamma_2+6R_2)^2}\right] \quad (43)$$

Hindered Rotators with a Known r_0

Fluorophores in lipid bilayers often display hindered rotational motions, which are revealed by nonzero anisotropy values (r_∞) at times much longer than the intensity decay times [37,51–53]. For the simple case of a single decay time and a single correlation time for the hindered motion,

$$I_\parallel(t) = \frac{1}{3}[(1+2r_\infty)e^{-\Gamma t} + 2(r_0 - r_\infty)e^{-(\Gamma+6R)t}] \quad (44)$$

$$I_\perp(t) = \frac{1}{3}[(1-r_\infty)e^{-\Gamma t} - (r_0 - r_\infty)e^{-(\Gamma+6R)t}] \quad (45)$$

Application of the transform equations, (14) and (15), yields

$$N_\parallel = \frac{1}{3}\left[\frac{(1+2r_\infty)\omega}{(\omega^2+\Gamma^2)} + \frac{2(r_0 - r_\infty)\omega}{\omega^2+(\Gamma+6R)^2}\right] \quad (46)$$

$$N_\perp = \frac{1}{3}\left[\frac{(1-r_\infty)\omega}{(\omega^2+\Gamma^2)} - \frac{(r_0 - r_\infty)\omega}{\omega^2+(\Gamma+6R)^2}\right] \quad (47)$$

$$D_\parallel = \frac{1}{3}\left[\frac{(1+2r_\infty)\Gamma}{(\omega^2+\Gamma^2)} + \frac{2(r_0 - r_\infty)(\Gamma+6R)}{\omega^2+(\Gamma+6R)^2}\right] \quad (48)$$

$$D_\perp = \frac{1}{3}\left[\frac{(1-r_\infty)\Gamma}{(\omega^2+\Gamma^2)} - \frac{(r_0 - r_\infty)(\Gamma+6R)}{\omega^2+(\Gamma+6R)^2}\right] \quad (49)$$

For this simple case of a single decay time and a single correlation time, one can obtain simple expressions for Δ_ω and Λ_ω using Eqs. (46)-(49) with Eqs. (12) and (13), yielding

$$\tan\Delta_\omega = \frac{3\omega\tau(r_0 - r_\infty)(6R\tau)}{m_0(1+\omega^2\tau^2) + S(6R\tau) + m_\infty(6R\tau)^2} \quad (50)$$

$$\Lambda_\omega = \sqrt{\frac{[(1+2r_0)\omega\tau]^2 + [1+2r_0+(1+2r_\infty)(6R\tau)]^2}{[(1-r_0)\omega\tau]^2 + [1-r_0+(1-r_\infty)(6R\tau)]^2}} \quad (51)$$

where $m_\infty = (1+2r_\infty)(1-r_\infty)$ and $S = 2 + r_0 - r_\infty(4r_0 - 1)$. The expression for Δ_ω has been described previously [54,55].

GLOBAL ANISOTROPY DECAY ANALYSIS

Global Anisotropy Analysis with Quenching

It is frequently difficult to obtain adequate resolution of complex anisotropy decays. One origin of this difficult is a mismatch between the correlation times and the intensity decay times. Hence, resolution of the anisotropy decay can be increased if the anisotropy data can be collected over a wider range of decay time. This can be accomplished by measurements of the anisotropy data for progressively quenched samples, followed by global analyses to recover a single anisotropy decay. The quenching can be any process which decreases the decay time, and we have used both collisional [16] and energy transfer [56] quenchers. The resolution is improved for several reasons, including measurements over a larger range of frequencies, measurements for a larger range of intensity decay times, and the availability of multiple data sets for the same physical process. The theory for global anisotropy analysis in the presence of quenching is conceptually simple. It is assumed that the quenching does not alter the anisotropy decay law, and alters only the intensity decay. Suppose these are measurements for q quencher concentrations. The intensity decay at each concentration of quencher [q] is analyzed to obtain the intensity decay, which is generally multi or nonexponential due to transient effects in quenching [18] or nonradiative energy transfer [56]. Hence, the intensity decay $I^q(t)$ and the α_i^q and τ_i^q values are known for each quenched sample. One then measures the FD anisotropy data for each of the quenched samples (Δ_ω^q and Δ_ω^q). These data are compared with the anisotropy data calculated ($\Delta_{c\omega}^q$ and $\Lambda_{c\omega}^q$) for an assumed anisotropy decay using the known values of α_i^q and τ_i^q for each quencher concentration. Hence, the analysis is unchanged except that the sum in Eq. (19) extends over both ω and q. As before, the value of r_0 can be fixed [Eqs. (40) and (41)] or variable [Eqs. (26)–(29)].

Multiple Excitation Wavelengths with Quenching

An alternative approach to obtaining increased resolution of an anisotropy decay is the use of multiple excitation wavelengths. Generally, the value of r_0 depends upon the excitation wavelength (λ). Since r_0 is a measure of the angle between the absorption and the emission transition moments, the use of different r_0 values results in different contributions of each rotational motion to the anisotropy decay. In general, one does not expect the rotational motions to be sensitive to the energy of the absorbed photons, so that the correlation

times will not depend upon the excitation wavelength (λ). The value of the fundamental anisotropy can be known from other experimental data [Eq. (52)] or unknown [Eq. (53)]. At each excitation wavelength (λ), the anisotropy decay is given by

$$r^{\lambda}(t) = r_0^{\lambda} \sum_j g_j e^{-t/\theta_j} \quad (r_0^{\lambda} \text{ known}) \tag{52}$$

$$r^{\lambda}(t) = \sum_j r_{0j}^{\lambda} e^{-t/\theta_j} \quad (r_0^{\lambda} \text{ unknown}) \tag{53}$$

It should be noted that there is a new set of anisotropy amplitudes r_{0i}^{λ} for each excitation wavelength. If there is a single data set at each wavelength, such as for measurements performed without quenching, then the anisotropy amplitudes are nonglobal, that is, determined by the single data set. If there is more than one data set at each excitation wavelength, such as data at several quencher concentrations, then the anisotropy amplitudes are partially global, being the same for the same excitation wavelength at all quencher concentrations.

One complication which arises in global analyses of anisotropy data is the possibility of different intensity decays for each excitation wavelength. For fluorophore fluid solvents, the intensity decays generally do not depend on the excitation wavelength. However, this is not generally true, particularly for solvent-sensitive fluorophores in environments of intermediate viscosity [57–61]. For such conditions the intensity decay can depend strongly on the excitation wavelength, particularly if the excitation is on the red (long-wavelength) edge of the absorption spectrum. For generality, it is best to assume that $I(t)$ is dependent upon excitation wavelength (λ) as well as quencher concentration [q]. Hence

$$I^{\lambda q}(t) = I_{\parallel}^{\lambda q}(t) + 2I_{\perp}^{\lambda q}(t) = \sum_i \alpha_i^{\lambda q} e^{-t/\tau_i^{q\lambda}} = \sum_i \alpha_i^{\lambda q} e^{-t\Gamma_i^{q\lambda}} \tag{54}$$

For this case the transforms must be calculated for each [q] and λ and are given by

$$N_p^{\lambda q} = \int I_p^{\lambda q}(t) \sin \omega t \, dt \tag{55}$$

$$D_p^{\lambda q} = \int I_p^{\lambda q}(t) \cos \omega t \, dt \tag{56}$$

The calculated values of Δ_ω and Λ_ω for each λ and [q] are given by

$$\Delta_{c\omega}^{\lambda q} = \arctan\left(\frac{D_{\parallel}^{\lambda q} N_{\perp}^{\lambda q} - N_{\parallel}^{\lambda q} D_{\perp}^{\lambda q}}{N_{\parallel}^{\lambda q} N_{\perp}^{\lambda q} + D_{\parallel}^{\lambda q} D_{\perp}^{\lambda q}}\right) \tag{57}$$

$$\Lambda_{c\omega}^{\lambda q} = \left(\frac{(N_{\parallel}^{\lambda q})^2 - (D_{\parallel}^{\lambda q})^2}{(N_{\perp}^{\lambda q})^2 + (D_{\perp}^{\lambda q})^2}\right)^{1/2} \tag{58}$$

The goodness of fit is calculated from the global χ_R^2,

$$\chi_R^2 = \frac{1}{\nu} \sum_{\omega,\lambda,q} \left(\frac{\Delta_\omega^{\lambda q} - \Delta_{c\omega}^{\lambda q}}{\delta\Delta}\right)^2 + \frac{1}{\nu} \sum_{\omega,\lambda,q} \left(\frac{\Lambda_\omega^{\lambda q} - \Lambda_{c\omega}^{\lambda q}}{\delta\Lambda}\right)^2 \tag{59}$$

where the sum extends over the modulation frequencies (ω), wavelengths (λ), and quencher concentrations (q). The transforms can be calculated from Eqs. (26)–(29) for each λ and [q]. For an unknown value of r_0 these terms are given by

$$A^{\lambda q} = \sum_i \frac{\alpha_i^{\lambda q} \omega}{\omega^2 + (\Gamma_i^{\lambda q})^2} \tag{60}$$

$$B^{\lambda q} = \sum_i \alpha_i^{\lambda q} \omega \sum_j \frac{r_{0j}^{\lambda}}{\omega^2 + (\Gamma_i^{\lambda q} + 6R_j)^2} \tag{61}$$

$$C^{\lambda q} = \sum_i \frac{\alpha_i^{\lambda q} \Gamma_i^{\lambda q}}{\omega^2 + (\Gamma_i^{\lambda q})^2} \tag{62}$$

$$D^{\lambda q} = \sum_i \alpha_i^{\lambda q} \sum_j \frac{r_{0j}^{\lambda} (\Gamma_i^{\lambda q} + 6R_j)}{\omega^2 + (\Gamma_i^{\lambda q} + 6R_j)^2} \tag{63}$$

We note that in these expressions [Eqs. (60)–(63)] the values of r_{0j}^{λ} are dependent on the excitation wavelength (λ), whereas the values of R_j are not wavelength dependent. The intensity decay parameters ($\alpha_i^{\lambda q}$ and Γ) are dependent on the quencher concentration (q) and, depending upon the probe and solvent conditions, may be dependent on the excitation wavelength (λ). Similar expressions apply if the r_0^{λ} values are known, except that the sum of the r_{0j}^{λ} values is held fixed at the known values, that is, $\Sigma r_{0jgi}^{\lambda} = r_0^{\lambda}$. At this point the explicit listing of examples seems unnecessary. It is now straightforward to write the explicit expression for any desired model. These expressions are easily written from Eqs. (60)–(63) and by recalling that the values of $\alpha_i^{\lambda q}$ and $\tau_i^{\lambda q}$ are specific for each data set.

COMPLEX ANISOTROPY DECAY MODELS

Associated Anisotropy Decays—Mixtures of Fluorophores

In all the proceeding sections we assumed that there was no association between the intensity decay times and the correlation times of the anisotropy decay. For a multiexponential model this means that the individual fluorophore species each display multiple decay times and multiple correlation times. However, it is possible that the fluorophore exists in two or more environments, each with a characteristic intensity decay and anisotropy de-

cay or, alternatively, that the sample contains two or more different fluorophores, each with a characteristic intensity decay and anisotropy decay time. The latter cases are called associated anisotropy decays because each intensity decay is associated with an anisotropy decay [41–43].

With the presently available resolution it is usually not practical to consider multiexponential intensity and anisotropy decays for each species in an associated system, so that it is more common to speak of the association between a single decay time with a single correlation time, rather than a multiexponential intensity decay with a multiexponential anisotropy decay. Hence, we limit the discussion to the case of a single decay rate and single correlation time for each species. For this associated model the anisotropy decay is given by

$$r(t) = \sum_k f_k(t)\, r_k(t) = \sum_k f_k(t)\, r_{0k}\, e^{-6R_k t} \quad (64)$$

where $r_k(t)$ is the single exponential anisotropy decay associated with the kth species in the sample. For this case of a mixture of fluorophores, each of which displays a single decay time, the intensity decay is given by

$$I(t) = \sum_k \gamma_k e^{-\tau_k t} \quad (65)$$

where γ_k represents the intensity at $t=0$ of the kth species and Γ_k its decay time ($\Gamma_k = \tau_k^{-1}$). For the case of the same fluorophore in two or more different environments, the radiative decay rates are typically the same, in which case the γ_k values represent the fractional population in each environment. At any point in time the fractional contribution of the kth species is given by

$$f_k(t) = \frac{\gamma_k e^{-\Gamma_k t}}{\sum_m \gamma_m e^{-\Gamma_m t}} \quad (66)$$

The terms needed to calculate the transforms are given by

$$B = \sum_k \frac{r_{0k}\, \gamma_k\, \omega}{\omega^2 + (\Gamma_k + 6R_k)^2} \quad (67)$$

$$D = \sum_k \frac{r_{0k}\, \gamma_k\, (\Gamma_k + 6R_k)}{\omega^2 + (\Gamma_k + 6R_k)^2} \quad (68)$$

where A and C are the same as Eqs. (26) and (28). Note that Eqs. (67) and (68) do not contain the cross-sums which are present in Eqs. (27) and (29) because each intensity decay k is associated with the correlation time k. For the case of two fluorophores the A and C terms are given by Eqs. (36) and (38), and

$$B = \frac{r_{01}\, \gamma_1\, \omega}{\omega^2 + (\Gamma_1 + 6R_1)^2} + \frac{r_{02}\, \gamma_2\, \omega}{\omega^2 + (\Gamma_2 + 6R_2)^2} \quad (69)$$

$$D = \frac{r_{01}\, \gamma_1\, (\Gamma_1 + 6R_1)}{\omega^2 + (\Gamma_1 + 6R_1)^2} + \frac{r_{02}\, \gamma_2\, (\Gamma_2 + 6R_2)}{\omega^2 + (\Gamma_2 + 6R_2)^2} \quad (70)$$

It is important to understand the meaning of the terms in this associated model. In Eqs. (69) and (70) the values r_{01} and r_{02} represent the fundamental anisotropies of the two species, and not partial amplitudes of a multiexponential decay as in the case of a nonassociated model. Similarly, R_1 and R_2 represent the rotational rates of the two species. The terms γ_1 and γ_2 represent the $t=0$ intensities of the two species.

This mixture model usually contains fewer variable parameters than does the nonassociated model. Depending upon the experimental system, it may be possible to measure the decay time of the fluorophore in each of the environments. In this case the values of Γ_1 and Γ_2 are known. Alternatively, the intensity decay sample displaying both decay times may be determined from a multiexponential analysis. In this case the values of γ_k and Γ_k are known. The data can be used to recover the θ_k and r_{0k} values. For a single fluorophore in two environments the values of r_{0k} are expected to be the same. Hence, if the Γ_k and r_{0k} values are known, then the FD anisotropy data can be used to calculate the value of the fractional amplitude γ_k [43].

Suppose now that the species in the mixture each display a more complex multiexponential intensity and anisotropy decay. The intensity decay of each species (k) is thus given by

$$I_k(t) = \sum_i \alpha_{ki}\, e^{-t/\tau_{ki}} \quad (71)$$

where α_{ki} is the ith component of the intensity decay of species k, and τ_{ki} is the decay time of this component. The anisotropy decay of each species is also assumed to be multiexponential,

$$r_k(t) = \sum_j r_{kj}\, e^{-t/\theta_{kj}} \quad (72)$$

where $r_k(t)$ is the anisotropy decay of the kth species, and θ_{kj} is the correlation time of this compound (j) in the anisotropy decay of the kth species.

It is important to be clear about the assumptions of this model. The model is associative in that the intensity decay of species k, $I_k(t)$, is associated with the anisotropy decay of species k, $r_k(t)$. However, we are assuming a

nonassociated model for the anisotropy decay of each species. The total intensity decay is given by

$$I(t) = \sum_k \gamma_k I_k(t) \tag{73}$$

where γ_k represents the fractional amplitude at $t=0$ of the total decay due to the kth species, $\Sigma_k \gamma_k = 1$. For the moment, we assume that the k species are due to the same fluorophores in k different environments. In this case we expect the radiative decay rates to be the same and the initial amplitudes to reflect the relative amounts of the fluorophore in each environment. For instance, consider a fluorophore to be partitional between two environments, free (F) and bound (B). Then, $\gamma_1 = C_F$ and $\gamma_2 = C_B$, where C_F and C_B are the concentrations of the free and bound forms, respectively.

The polarized components of the intensity decay for each species are given by

$$I_{k\parallel}(t) = \frac{1}{3} I_k(t) \left[1 + 2r_k(t)\right] \tag{74}$$

$$I_{k\perp}(t) = \frac{1}{3} I_k(t) \left[1 - r_k(t)\right] \tag{75}$$

More explicitly, with $\Gamma_{ki} = \tau_{ki}^{-1}$ and $6R_{kj} = \theta^{-1}$, one obtains

$$I_{k\parallel}(t) = \frac{1}{3} \sum_i \alpha_{ki} e^{-\Gamma_{ki} t} + \frac{2}{3} \sum_i \sum_j \alpha_{ki} r_{kj} e^{-(\Gamma_{ki} + 6R_{kj})t} \tag{76}$$

$$I_{k\perp}(t) = \frac{1}{3} \sum_i \alpha_{ki} e^{-\Gamma_{ki} t} - \frac{1}{3} \sum_i \sum_j \alpha_{ki} r_{kj} e^{-(\Gamma_{ki} + 6R_{kj})t} \tag{77}$$

The total intensity of each polarized component is given by

$$I_\parallel(t) = \sum_k \gamma_k I_{k\parallel}(t) \tag{78}$$

$$I_\perp(t) = \sum_k \gamma_k I_{k\perp}(t) \tag{79}$$

After Fourier transformation of Eqs. (78) and (79) with $I_{k\parallel}$ and $I_{k\perp}$ given by Eqs. (76) and (77), one obtains expressions for $N_\parallel$, $N_\perp$, $D_\parallel$, and $D_\perp$ which have the same form as Eqs. (22)–(25). However, the quantities A, B, C, and D now have more complicated forms:

$$A = \sum_k \sum_i \frac{\gamma_k \alpha_{ki} \omega}{\omega^2 + \Gamma_{ki}^2} \tag{80}$$

$$B = \sum_k \sum_i \sum_j \frac{\gamma_k \alpha_{ki} r_{kj} \omega}{\omega^2 + (\Gamma_{ki}^2 + 6R_{kj})^2} \tag{81}$$

$$C = \sum_k \sum_i \frac{\gamma_k \alpha_{ki} \Gamma_{ki}}{\omega^2 + \Gamma_{ki}^2} \tag{82}$$

$$D = \sum_k \sum_i \sum_j \frac{\gamma_k \alpha_{ki} r_{kj} (\Gamma_{ki} + 6R_{kj})}{\omega^2 + (\Gamma_{ki}^2 + 6R_{kj})^2} \tag{83}$$

For clarity it seems best to write an explicit expansion of Eq. (22). For the case of two species (k = 1,2), each with two decay times (i = 1,2) and two correlation times (j = 1,2), we have

$$\begin{aligned} N_\parallel(t) = {} & \frac{\gamma_1 \omega}{3} \left(\frac{\alpha_{11}}{\omega^2 + \Gamma_{11}^2} + \frac{\alpha_{12}}{\omega^2 + \Gamma_{12}^2} \right) \\ & + \frac{\gamma_2 \omega}{3} \left(\frac{\alpha_{21}}{\omega^2 + \Gamma_{21}^2} + \frac{\alpha_{22}}{\omega^2 + \Gamma_{22}^2} \right) \\ & + \frac{2\gamma_1 \omega}{3} \left[\alpha_{11} \left(\frac{r_{11}}{\omega^2 + (\Gamma_{11} + 6R_{11})^2} + \frac{r_{12}}{\omega^2 + (\Gamma_{11} + 6R_{12})^2} \right) \right. \\ & \left. + \alpha_{12} \left(\frac{r_{11}}{\omega^2 + (\Gamma_{12} + 6R_{11})^2} + \frac{r_{12}}{\omega^2 + (\Gamma_{12} + 6R_{12})^2} \right) \right] \\ & + \frac{2\gamma_2 \omega}{3} \left[\alpha_{21} \left(\frac{r_{21}}{\omega^2 + (\Gamma_{21} + 6R_{21})^2} + \frac{r_{22}}{\omega^2 + (\Gamma_{21} + 6R_{22})^2} \right) \right. \\ & \left. + \alpha_{22} \left(\frac{r_{21}}{\omega^2 + (\Gamma_{22} + 6R_{21})^2} + \frac{r_{22}}{\omega^2 + (\Gamma_{22} + 6R_{22})^2} \right) \right] \end{aligned} \tag{84}$$

We note that a complete resolution of the multiple intensity decay and correlation times for such a system is a formidable task. The resolution may be simplified by adding information, from other experiments, which fix some of the parameters. For instance, in the case of a two-species model, it may be possible to determine independently the intensity decay (α_{ki} and τ_{ki}) and anisotropy decay (r_{kj} and θ_{kj}) law. In this case the only remaining parameter would be the amplitude (or concentration) of each species (C_k).

Distributions of Correlation Times

In all the above models we assumed that the anisotropy decays are a sum of exponentials. However, there are many situations where the anisotropy decay is known to be nonexponential, such as for dyes intercalated into DNA [62–64] or probes embedded in the anisotropies and hindered environment of a membrane [65,66]. By analogy, it seems probable that the anisotropy decays of tryptophan residue in proteins may also be nonexponential since these two exist in a hindered environment. In fact, experimental studies of the anisotropy decay of proteins [67–73] and molecular dynamics calculations [74–75] have shown that the tryptophan anisotropy decays often show the properties of hindered motions.

The cases described above could be described in terms of the distribution of correlation times. The shapes of the distribution would indicate the time ranges where most of the motions occur. Hence, as a final model we

describe the formalism for analysis of FD anisotropy data in terms of the distribution of correlation times.

To describe the distributions we assume that each mode (kj) of the distribution is described by a mean (θ_{kj}) of the distribution and full-width at half-maximal intensity (hw_{kj}), which in turn are described by normalized probability functions [$P_{kj}(\theta)$]. These can be Gaussian (G), Lorentzian (L), or other functions. For these two cases

$$P_{kj}^{G}(\theta) = \begin{cases} \frac{1}{Z_G} \exp\left(-\frac{\theta - \theta_{kj})^2}{2\sigma_{kj}^2}\right) & \text{for } \theta \geq 0 \\ 0 & \text{for } \theta < 0 \end{cases} \quad (85)$$

$$P_{kj}^{L}(\theta) = \begin{cases} \frac{1}{Z_L} \frac{hw_{kj}/2}{(\theta - \theta_{kj})^2 + (hw_{kj}/2)^2} & \text{for } \theta \geq 0 \\ 0 & \text{for } \theta < 0 \end{cases} \quad (86)$$

where σ_{kj} is the standard deviation of the untruncated Gaussian and Z_G and Z_L are the normalization factors defined as

$$Z_G = \int_0^\infty \exp\left(-\frac{(\theta - \theta_{kj})^2}{2\sigma_{kj}^2}\right) d\theta \quad (87)$$

$$Z_L = \int_0^\infty \frac{hw_{kj}/2}{(\theta - \theta_{kj})^2 + (hw_{kj}/2)^2} d\theta \quad (88)$$

The half-width of the Gaussian (hw_{kj}) is related to its σ_{kj} by $hw_{kj} = 2.355\ \sigma_{kj}$. For such an anisotropy decay time distribution there is an amplitude at correlation time θ which is given by

$$r_k(t, \theta) = \sum_j r_{kj} P_{kj}(\theta)\, e^{-t/\theta} \quad (89)$$

We note that for a given correlation time θ there may be contributions from more than one mode of the distribution. One cannot directly observe the anisotropy decay for a given correlation time but, rather, observes the entire anisotropy decay, which is given by the integral of Eq. (89) over theta,

$$r_k(t) = \int_0^\infty r_k(t, \theta)\, d\theta \quad (90)$$

The values of $N_\parallel$, $N_\perp$, $D_\parallel$, and $D_\perp$ are calculated using Eqs. (22)–(25) with quantities A and C given by Eqs. (80) and (82). The exprressions for B and D now have the form

$$B = \sum_k \sum_i \sum_j \int_0^\infty \frac{\gamma_k \alpha_{ki} r_{kj} \omega P_{kj}(\theta)}{\omega^2 + (\Gamma_{ki}^2 + 6R_{kj})^2} d\theta \quad (91)$$

$$D = \sum_k \sum_i \sum_j \int_0^\infty \frac{\gamma_k \alpha_{ki} r_{kj} (\Gamma_{ki} + 6R_{kj}) P_{kj}(\theta)}{\omega^2 + (\Gamma_{ki}^2 + 6R_{kj})^2} d\theta \quad (92)$$

It should be noted that in the above expressions parameter θ is also involved in terms $6R_{kj}$ by the relation $6R_{kj} = \theta^{-1}$.

SUMMARY

In this review we summarize the expressions needed to analyze FD anisotropy data. Expressions are provided for single- and multiexponential intensity and anisotropy decays, as these apply to the usual nonassociated decays and to associated anisotropy decays. And finally, we discuss correlation time distribution, which can allow visualization of dynamic processes in macromolecules.

ACKNOWLEDGMENTS

This work was supported by National Science Foundation Grants DMB-8804931 and DIR-8710401 and National Institute of Health Grants RR-08119 and RR-07510. J.R.L. acknowledges support from the Medical Biotechnology Center at the University of Maryland. The authors express appreciation to Drs. R. Jayaweera and H. Szmacinski for assistance in developing the theory and analysis procedures for mixtures of fluorophores.

NOMENCLATURE

$\parallel$	Parallel
$\perp$	Perpendicular
$I(t)$	Intensity decay
α_i	Preexponential factor in the intensity decay
τ_i	Decay time in the intensity decay
Γ_i	Decay rate $= (\tau_i)^{-1}$ in the intensity decay
θ_j	Correlation time $= (6\ R_j)^{-1}$ in the anisotropy decay
R_j	Rotational rate in the anisotropy decay
r_0	Fundamental anisotropy
g_j	Fractional amplitude in the anisotropy decay
r_{0j}	Total amplitude in the anisotropy decay
χ_R^2	Sum of the squared and weighted deviations
$P^G(\theta)$	Gaussian distribution of correlation time
$P^L(\theta)$	Lorentzian distribution of correlation time
$r(t)$	Anisotropy decay

Subscripts

c	Calculated value

k kth species

REFERENCES

1. G. G. Belford, R. L. Belford, and G. Weber (1972) *Proc. Natl. Acad. Sci.* **69,** 1392–1393.
2. T. J. Chuang and K. B. Eisenthal (1972) *J. Chem. Phys.* **57,** 5094–5097.
3. M. Ehrenberg and R. Rigler (1972) *Chem. Phys. Lett.* **14,** 539–544.
4. R. F. Steiner (1983) in R. F. Steiner (Ed.), *Excited States of Biopolymers,* Plenum Press, New York, pp. 117–162.
5. I. Munro, I. Pecht, and L. Stryer (1979) *Proc. Natl. Acad. Sci.* **65,** 823–830.
6. J. Yguerabide, H. F. Epstein, and L. Stryer (1979) *J. Mol. Biol.* **51,** 573–590.
7. R. D. Ludescher, I. D. Johnson, J. J. Volwerk, G. H. de Haas, P. C. Jost, and B. S. Hudson (1988) *Biochemistry* **27,** 6618–6628.
8. D. R. James, D. R. Demmer, R. P. Steer, and R. T. Verral (1985) *Biochemistry* **24,** 5517–5526.
9. A. D. MacKerell, R. Rigler, L. Nilsson, N. Hahn, and W. Saenger (1987) *Biophys. Chem.* **26,** 247–261.
10. T. M. Nordlund and D. M. Podolski (1983) *Photochem. Photobiol.* **38,** 665–669.
11. E. Jahn and F. Jahnig (1988) *Biophys. J.* **54,** 817–827.
12. F. Claesens and R. Rigler (1986) *Eur. J. Biochim.* **13,** 331–342.
13. L. X. Q. Chen, J. W. Longworth, and G. R. Fleming (1987) *Biophys. J.* **51,** 865–873.
14. J. R. Lakowicz, I. Gryczyński, H. Szmacinski, H. Cherek, and N. Joshi (1991) *Eur. Biophys. J.* **19,** 125–140.
15. R. F. Steiner (1991) in J. R. Lakowicz (Ed.), *Topics in Fluorescence Spectroscopy, Vol. 2. Principles,* Plenum Press, New York, pp. 1–52.
16. J. R. Lakowicz, E. Gratton, G. Laczko, H. Cherek, and M. Limkeman (1984) *Biophys. J.* **46,** 463–467.
17. J. R. Lakowicz, H. Cherek, I. Gryczynski, N. Joshi, and M. L. Johnson (1987) *Biophys. Chem.* **28,** 35–50.
18. J. R. Lakowicz, M. L. Johnson, I. Gryczynski, N. Joshi, and G. Laczko (1987) *J. Phys. Chem.* **91,** 3277–3285.
19. E. Gratton, M. Limkeman, J. R. Lakowicz, B. Maliwal, H. Cherek, and G. Laczko (1984) *Biophys. J.* **46,** 479–486.
20. J. R. Lakowicz and I. Gryczynski (1991) *Topics in Fluorescence Spectroscopy, Vol 1. Techniques,* Plenum Press, New York, pp. 293–335.
21. J. R. Lakowicz, I. Gryczynski, and H. Cherek (1986) *J. Biol. Chem.* **261,** 2240–2245.
22. B. P. Maliwal and J. R. Lakowicz (1986) *Biochim. Biophys. Acta* **873,** 173–181.
23. J. R. Lakowicz, G. Laczko, and I. Gryczynski (1987) *Biochemistry* **26,** 82–90.
24. I. Gryczynski, H. Cherek, and J. R. Lakowicz (1988) *Biophys. Chem.* **30,** 271–277.
25. J. R. Lakowicz and I. Gryczynski (1992) *Arab. J. Sci. Eng.* **17,** 261–286.
26. I. Gryczynski, H. Cherek, and J. R. Lakowicz (1988) *Biophys. Chem.* **30,** 271–277.
27. D. M. Jameson and E. Gratton (1983) in D. Eastwood (Ed.), *New Directions in Molecular Luminescence,* ASTM STP 882, pp. 67–81.
28. J. R. Alcala, E. Gratton, and F. C. Prendergast (1987) *Biophys. J.* **51,** 587–596.
29. R. D. Spencer and G. Weber (1979) *J. Chem. Phys.* **52,** 1654–1663.
30. H. Merkelo, J. H. Hammond, S. R. Hartman, and Z. I. Derzko (1970) *J. Luminesc.* **1**(2), 502–512.
31. G. Weber (1977) *J. Chem. Phys.* **66,** 4081–4091.
32. P. R. Bevington (1969) *Data Reduction and Error Analysis for the Physical Sciences,* McGraw-Hill, New York.
33. M. L. Johnson (1983) *Biophys. J.* **44,** 101–106.
34. M. L. Johnson and S. G. Frasier (1985) *Methods Enzymol.* **117,** 301–342.
35. M. G. Bedea and L. Brand (1979) *Methods Enzymol.* **61,** 378–425.
36. A. J. Cross and G. R. Fleming (1984) *Biophys. J.* **46,** 45–56.
37. R. E. Dale, L. A. Chen, and L. Brand (1977) *J. Biol. Chem.* **252,** 7500–7510.
38. M. C. Chang, S. H. Courtney, A. J. Cross, R. J. Gulathy, J. W. Petrich, and G. R. Fleming (1985) *Anal Instrument* **14,** 433–464.
39. D. V. O'Connor and D. Phillips (1984) *Time-correlated Single Photon Counting,* Academic Press, Orlando, pp. 256–261.
40. J. R. Lakowicz (1983) *Principles of Fluorescence Spectroscopy,* Plenum Press, New York, pp. 111–181.
41. J. R. Knutson, L. Davenport, and L. Brand (1986) *Biochemistry* **25,** 1805–1810.
42. L. Davenport, J. R. Knutson, and L. Brand (1986) *Biochemistry* **25,** 1811–1816.
43. H. Szmacinski, R. Jayaweera, H. Cherek, and J. R. Lakowicz (1987) *Biophys. Chem.* **27,** 233–241.
44. J. R. Lakowicz, H. Cherek, I. Gryczynski, N. Joshi, and M. L. Johnson (1987) *Biophys. J.* **51,** 755–768.
45. I. Gryczynski, H. Cherek, G. Laczko, and J. R. Lakowicz (1987) *Chem. Phys. Lett.* **135,** 193–197.
46. J. R. Taylor (1982) *An Introduction to Error Analysis: The Study of Uncertainties in Physical Measurements,* University Science Books, Mill Valley, California.
47. G. Weber (1966) in D. M. Hercules (Ed.), *Fluorescence and Phosphorescence Analysis,* pp. 217–240.
48. M. Shinitzky, A. C. Dianoux, C. Gitler, and G. Weber (1971) *Biochemistry* **10,** 2106–2113.
49. J. R. Lakowicz, B. P. Maliwal, H. Cherek, and A. Balter (1983) *Biochemistry* **22,** 1741–1752.
50. B. Valuer and G. Weber (1977) *Photochem. Photobiol.* **25,** 441–444.
51. S. Kawato, K. Kinosita, and A. Ikegami (1977) *Biochemistry* **16,** 2319–2324.
52. F. Jahnig (1979) *Proc. Natl. Acad. Sci.* **76,** 6361–6365.
53. W. R. Veach and L. Stryer (1977) *J. Mol. Biol.* **177,** 1109–1113.
54. G. Weber (1978) *Acta Phys. Palonica* **A54,** 859–865.
55. J. R. Lakowicz, F. G. Prendergast, and D. Hogen (1979) *Biochemistry* **18,** 508–519.
56. J. R. Lakowicz, I. Gryczynski, and W. Wiczk (1988) *Chem. Phys. Lett.* **149,** 134–139.
57. A. N. Rubinov, V. I. Tomin, and B. A. Bushuk (1982) *J. Luminesc.* **26,** 377–391.
58. L. V. Levshin, I. A. Stuganov, and B. N. Toleutaev (1988) *Opt. Spectrosc.* **64,** 186–189.
59. L. V. Levshin, I. A. Stuganov, and B. N. Toleutaev (1988) *Opt. Spectrosc.* **64,** 323–325.
60. J. R. Lakowicz and S. Keating (1984) *Biochemistry* **23,** 3013–3021.
61. A. P. Demchenko (1986) *Ultraviolet Spectroscopy of Proteins,* Springer-Verlag, Berlin, pp. 145–172.
62. M. D. Barkley and B. H. Zimm (1979) *J. Chem. Phys.* **70,** 2291–3007.
63. J. M. Schurr (1984) *Chem. Phys.* **84,** 71–96.
64. J. M. Schurr, B. S. Fujimoto, P. Wu, and L. Song (1992) *Topics in Fluorescence Spectroscopy, Vol. 3. Biochemical Applications,* Plenum Press, New York, pp. 137–229.
65. R. E. Dale, L. A. Chen, and L. Brand (1977) *J. Biol. Chem.* **252,** 7500–7510.
66. K. Kinosita, S. Kawato, and A. Ikegami (1977) *J. Biophys.* **20,** 289–305.

67. I. Munro, I. Pecht, and L. Stryer (1979) *Proc. Natl. Acad. Sci.* **76,** 56–60.
68. J. M. Beechem and L. Brand (1985) Ann. Rev. Biochem. **54,** 43–71.
69. L. X. Chen, J. W. Longworth, and G. R. Fleming (1987) *Biophys. J.* **51,** 865–873.
70. T. M. Nordlund and D. A. Podolski (1983) *Photochem Photobiol.* **38,** 665–669.
71. T. M. Nordlund, X. Y. Liu, and J. H. Sommer (1986) *Proc. Natl. Acad. Sci.* **83,** 8977–8981.
72. J. W. Petrich, J. W. Longworth, and G. R. Fleming (1987) *Biochemistry* **26,** 2711–2722.
73. T. Kouyama, K. Kinosita, and A. Ikegami (1989) *Eur. J. Biochem.* **182,** 517–521.
74. I. Ghosh and J. A. McCammon (1987) *Biophys. J.* **51,** 637–641.
75. D. L. Harris and B. S. Hudson (1991) *Chem. Phys.* **158,** 353–382.